Shatat, Mahmood and Riffat, Saffa and Gan, Guohui (2016) An innovative psychometric solar-powered water desalination system. International Journal of Low-Carbon Technologies, 11 (2). pp. 254-265. ISSN 1748-1325

An innovative psychometric solar-powered water desalination system

Mahmoud Shatat*, **Saffa Riffat and Guohui Gan**

Department of Architecture and Built Environment, University of Nottingham, Nottingham NG7 2RD, UK

Abstract

Important advances have been made in solar water desalination technology but their wide application is restricted by relatively high capital and running costs. Until recently, solar concentrator collectors had usually been employed to distill water in compact desalination systems. Currently, it is possible to replace these collectors by the more efficient evacuated tube collectors, which are now widely available on the market at lower prices. This paper describes the results of experimental and theoretical investigations of the operation of a novel small-scale solar water desalination technology using the psychometric humidification and dehumidification process coupled with a heat pipe evacuated tube solar collector with an aperture area of ~1.73 m^2. Solar radiation during spring in the Middle East was simulated by an array of halogen floodlights. A synthetic brackish water solution was used for the tests and its total dissolved solids (TDSs) and electrical conductivity were measured. A mathematical model was developed to describe the system's operation. A computer program was written to solve the system of governing equations to perform the theoretical calculations of the humidification and dehumidification processes. The experimental and theoretical values for the total daily distillate output were found to be closely correlated. The test results demonstrate that, at temperatures of 55–60°C, the system produces ~5–6 kg/h of clean water with a high desalination efficiency. Following the experimental calibration of the mathematical model, it was demonstrated that the performance of the system could be improved to produce a considerably higher amount of fresh water.

*Corresponding author: mahmoodshatat@hotmail.com

Keywords: solar desalination; humidification; dehumidification; solar simulator

Received 25 June 2012; revised 12 September 2012; accepted 22 October 2012

1. INTRODUCTION

Many countries around the world, especially developing countries and countries in the Middle East, suffer from a shortage of fresh water. The United Nations Environment Programme (UNEP) stated that one-third of the world's population lives in countries with insufficient fresh water to support the population and, by 2025, two-thirds of the world population will face water scarcity [1]. Consequently, drinking water of an acceptable quality has become a scarce commodity. The total global water reserves are ~1.4 billion km^3; of which around 97.5% is in the oceans and the remaining 2.5% is fresh water present in the atmosphere, ice mountains and ground water. Of the total, only ~0.014% is directly available for human beings and other organisms [2]. Thermal solar energy water desalination is known to be a viable method of producing fresh water from saline water [2] in remote locations; humidification and dehumidification solar water desalinations units and conventional basin solar stills with a relatively large footprint are an example of such simple technology.

There are extensive R&D activities to find new and feasible methods of producing drinking water using renewable energy technologies [3]. Conventional desalination systems are operated with fossil fuel, which is becoming uneconomical and causes environmental pollution. In spite of these problems, it is likely that seawater desalination in large-scale heat and power plants will continue to play an essential role in providing fresh water for domestic and industrial use in areas of high population density in the Middle East. However, such plants are not economically viable in remote areas, even those near a coast, and an electricity supply can also be lacking. The development of alternative, compact, small-scale water desalination systems is imperative for the population in such areas [4]. A significant number of publications have focused on improving the design and performance of small-scale solar water desalination. For example, conventional basin solar stills without

International Journal of Low-Carbon Technologies 2016, 11, 254–265

doi:10.1093/ijlct/cts075 Advance Access Publication 13 December 2012

additional concentration of solar energy produce an average water output capacity of $\sim$2.5–3.0 l/m^2/day and their maximum thermal efficiency is around 25% because of large heat losses [5, 6].

The effect of coupling a flat plate solar collector with humidification and dehumidification processes and a basin solar still has also been investigated in a series of R&D projects. For example, Zhang and Yuan [7] studied a closed circulation solar desalination unit and focused on an analysis of water production and system performance by investigating the effects of the cooling water flow rate, the feed water rate and the structural dimensions. Similarly, Mohamed and El-Minshawy [8] and Eames *et al.* [9] described the theoretical and experimental investigation of a small-scale solar-powered barometric desalination system. Comparing the results with the given theory, they showed that the production rate of fresh water depended on three main factors, namely, the heat exchange effectiveness of the condenser, solar insolation and pressure. Mohamed and El-Minshawy [10] studied the same concept but with the use of geothermal energy. Gude *et al.* [11] studied low-temperature desalination using solar collectors of area 18 m^2 augmented by a thermal energy storage of 3 m^3; their work included theoretical and experimental investigation with a water production of 100 l/day.

Hou and Zhang [12] proposed a hybrid desalination process in a multi-effect humidification–dehumidification system heated by solar collectors and showed that the distilled water output ratio increased by a factor of 2–3 when the rejected water was reused. In this study, they maximized condenser heat recovery through composite curves and found that there is an optimum value for the water to air flow rate ratio, but they did not take the effect of the humidifier inlet temperature and the solar collector efficiency into account. Garg *et al.* [13] tested an MEH solar system to provide continuous hot water to a desalination unit over a 24 h period by system modeling based on solving heat and mass transfer equations. The result showed that the rate of distilled water production varied linearly as a function of water temperature at the humidifier. Similarly, Muller-Holst *et al.* [14] studied the same concept on a small-scale thermal seawater desalination apparatus and showed that the water productivity depended on the magnitude of the thermal energy used in the evaporation process. Soufari and Zamen [15] studied parametric effects on the performance of an HDD system and optimized the operating parameters. These studies show that an HDD system may operate at a temperature as low as 50°C, and therefore could be suitable for incorporation with a Rankine cycle power generation system. However, water quality should be taken into account because biological contamination can occur at low operating temperatures. Two solar desalination units of different sizes and both utilizing the concept of humidification and dehumidification were constructed in Jordan by Farid *et al.* [16] and Alhallaj *et al.* [17]. They found that the effect on the heat and mass transfer coefficients of the water flow rate is more significant than the effect of the air flow rate.

Utilizing the concept of humidification and dehumidification in water desalination in a compact unit coupled with solar collectors would have a significant improvement on water production, and owing to its high efficiency, the possibility of directly integrating it with a renewable energy source and its lower maintenance and technical support needs, it can be considered a unique thermal technique for small-scale applications. Hence, this research aims to develop a novel desalination system that is more affordable because it requires a very small energy input. It uses the hybrid Psychometric Energy Process Desalination system based on the humidification and dehumidification principle with two specially designed humidifiers to increase the waste heat recovery efficiency. This system is also connected with an evacuated solar collector panel. Unlike most previous experimental and simulation work that was restricted to steady-state operation at a fixed value of insolation, this work will describe the experimental results and the mathematical model of the psychometric process with evaporation and condensation for transient numerical simulations for insolation variations over the daylight and extended overnight periods. Furthermore, experimental investigations will no longer be restricted to a specific solar insolation region because the light solar simulator developed as part of this research makes it possible to simulate solar insolation conditions anywhere in the world.

2. SYSTEM DESCRIPTION

A novel water desalination system was developed at the Institute of Sustainable Energy Laboratories at University of Nottingham. This system employs the concept of humidification and dehumidification based on the pyschrometric energy process using a specially designed heat recovery system converting saline water into fresh water. Figure 1 shows a schematic diagram of the desalination system.

This system includes the water desalination unit and the heat source, which can be either an electric heating coil submerged into a rectangular water storage tank or an evacuated solar collector with circulation pumps, air fan and auxiliary components. The desalination unit consists of primary and secondary humidification chambers for humidifying the moist air and improving heat recovery, respectively. The dehumidification chamber contains a well-designed heat exchanger, where condensation and recovery of the latent heat of condensation take place for energy recycling and water production, respectively.

The key innovation is the reuse of the latent heat from the condensing moisture in the carrier gas: only a little thermal energy is supplied to the humidification and dehumidification process. The HDD system can be one-stage or multi-stage.

The dehumidifier with the condenser serves as an efficient agent for the processes of condensation and heat recovery. The seawater or brackish cooling water is pumped from the water storage tank, which is located at the bottom of the secondary humidification chamber, and passes through the dehumidifier to the secondary humidification chamber again in order to humidify the incoming air where the cooling seawater and fresh air are mixed in order to aid evaporation and to recover the waste heat of condensation. At the same time, they aid in the condensation process by extracting heat from the vapor. Therefore, most of the heat in the system is utilized to produce fresh water. The moist air is then transferred from the secondary humidification chamber to the second primary humidifier, where the air is further humidified by the circulation of sprayed hot salty water. Both humidification chambers consist of porous media made of cellulose material and a single-tube water sprayer. It has a dimension of $0.7 \times 0.5 \times 0.2$ m where the pad humidifier unit is made of a rectangular cassette of corrugated cellulose packing material. The exiting moist air vapor then passes through the condenser to be dehumidified and leaves the system as exhaust air and condensed fresh water.

The desalination unit is connected to a 120 l storage tank through the humidifier with a circulation pump and a flow meter regulator to adjust the mass flow rate of hot water. This storage tank is fully insulated with foam insulation materials to reduce the heat losses and to keep the system running during the night utilizing the heat stored from solar energy during the day. The water inside the storage tank is heated by a helical copper tubular heat exchanger. The inlet and outlet of the heat exchanger are connected, respectively, to the outlet and the inlet of the manifold at the top of evacuated solar collector with an area of $\sim$2.02 m^2 so that these form a closed loop and an electrical pump circulates the water in the loop. The copper manifold header pipe of the collector is a long horizontal cylinder with a volume of $\sim$0.45 l. The header pipe also contains 20 small cylindrical heat pipe housing ports. The axis of each housing port is perpendicular to the flow direction in the header pipe. In the solar collector, the head of each evacuated tube heat pipe is inserted into a separate housing port and the heat from the header pipes is transferred to the flow inside the header pipe through the walls of the housing ports. The thermal contact between the heads of the heat pipes and the housing ports is provided by using a special metallic glue compound. An expansion vessel is also incorporated into the system in order to prevent the possibility of system damage due to an increase in pressure, and the fluid pressure in the solar collector manifold is monitored by a pressure gauge, as illustrated in Figure 2.

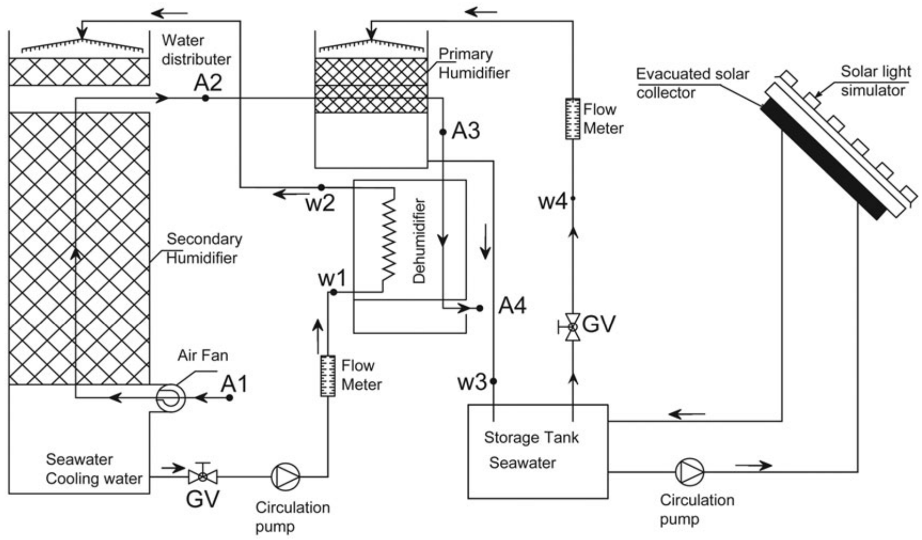

Figure 1. *Schematic diagram for the desalination system.*

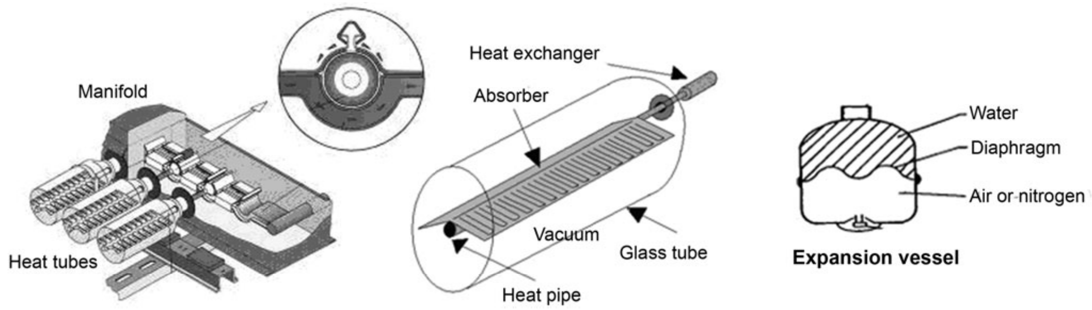

Figure 2. *Evacuated solar collector manifolds and heat tubes assembly [19].*

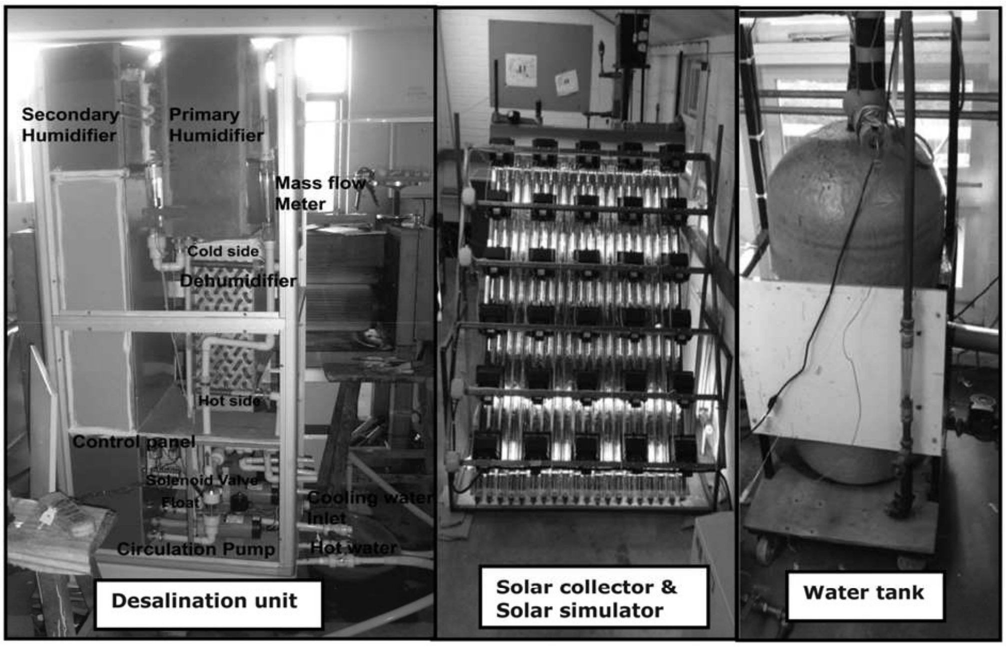

Figure 3. *Experimental test rig [Desalination unit—solar collector covered with solar simulator—Storage tank].*

An array of 30 halogen floodlights is used as a solar sunlight simulator. The floodlights are evenly spaced on a frame installed above and in parallel to the evacuated tubes, as shown in Figure 3. The array is divided into three groups and is connected to the grid via a 3-phase transformer, which enables the level of the radiation flux to be gradually regulated. The maximum electrical power consumed by each floodlight is 400 W. A pyronometer with sensitivity of 17.99×10^{-6} V/W/m^2 measures the radiation flux at 20 different locations on the surface of the evacuated tubes and in the spaces between them. The results are averaged. The test rig is also equipped with a metered cylinder tank, circulation pumps and a set of K-type thermocouples to measure the temperature of the water circulating in the heated circuit and the temperature of the saline water at different points in the system. An anemometer device measures the air flow velocity and water flow meters measure the flow of the saline hot water, the cooling water and the fluid inside the solar collector manifold.

3. WORKING PRINCIPLE

In the schematic diagram system in Figure 1, the supplied energy is initially generated by the immersed electric heater of 2.5 kW in the water storage tank and then the system was connected with an evacuated solar collector. First, the energy absorbed is utilized to increase the temperature of the liquid which is continuously circulating in the humidifier of the desalination unit. The temperature of the saline water in the tank increases gradually and then the saline hot water is sprayed into the primary humidification chamber to humidify the incoming air. The process of humidification and dehumidification goes through four stages.

(1) The outside air at point 1 gets humidified in the primary evaporation chamber to become point 2; the energy required is supplied from the latent heat of water condensation recovered by cooling water in the condensation chamber so that most of the energy needed for desalination is reused. (2) The circulating air at point 2 passes through the primary humidification chamber 2 to get more humidified further to become point 3. (3) Air at point 3 passes through the condensing chamber of the HE to get dehumidified. (4) The air is discharged as exhaust, leaving the condensed water produced to be collected in the metering cylinder.

4. EXPERIMENTAL SETUP AND TEST PROCEDURE

The main components of the desalination system described in the previous section were designed and assembled as shown in Figure 3. Preliminary investigation trials were carried out on two stages of investigations. In the first stage, an electric heater was used as an energy source to heat the seawater in the storage tank but, in the second stage, the energy source was an integral evacuated solar collector.

All experimental parameters, such as temperature, air flow, water flow and relative humidity, were measured and recorded using a data logger (DT500). Temperatures were measured using K-type thermocouples with an accuracy of 0.1°C. Relative humidity was calculated on the basis of the measured dry bulb and wet bulb temperatures. The sensors were calibrated using a mercury-in-glass thermometer with ± 1 division accuracy. They were also immersed in a hot water bath and the same readings were obtained. The accuracy of the thermometer was checked with a handheld mercury thermometer which has an accuracy of 0.1°C. An anemometer was used to measure the exhaust air velocity in the desalination unit.

The desalination system was covered by thermo-insulation materials 25 mm in thickness. The synthetic brackish water with a high level of total dissolved solids (TDSs) and electrical conductivity was prepared and used to fill the storage tank. The evacuated solar collector with the storage tank system was tested in conditions simulating a typical spring semester in the Middle East. For this, information on the variation of the solar radiation during spring 2004 was used, as shown in Figure 4. The voltage level of electrical power supplied to floodlights was changed every 20 min using the floodlight irradiation measurement results presented in Figure 5.

The system was investigated under different hot water and cooling water mass flow rates and with various air flow rates. The fluid mass flow rate through the collector was kept at 180 kg/h, as recommended by the manufacturer. The tests were repeated several times and the water that condensed during the experiments was collected into a metering cylinder and measured after a 24 h period. To speed up the experimental investigation, an electric heater was used to heat up the salty water in the storage tank.

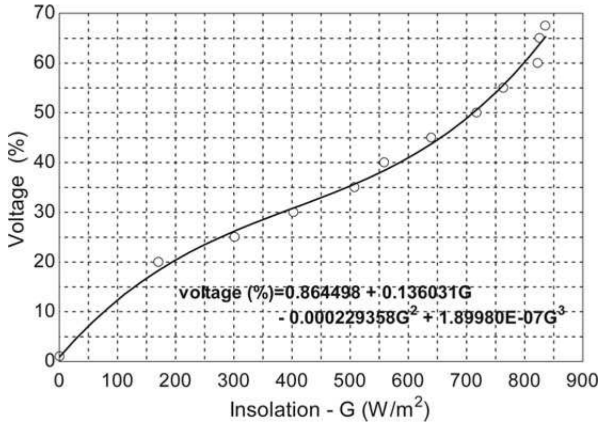

Figure 4. *Radiation level versus transformer voltage calibration results.*

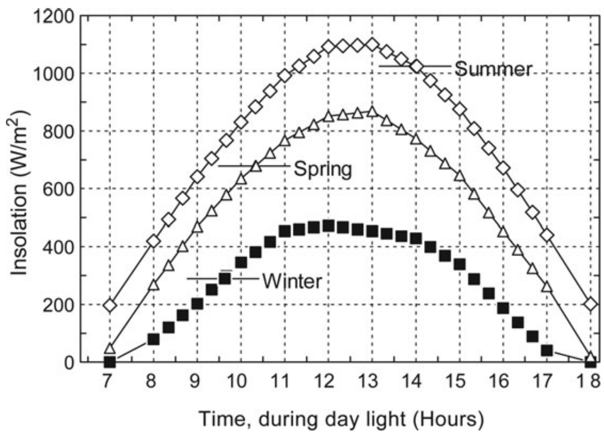

Figure 5. *Solar insolation variation in the Middle East.*

5. MATHEMATICAL MODEL

The mathematical model presented here shows the energy and mass conservation equations written for each part of the system. Figure 1 illustrates the behavior of the humidification and the dehumidification processes for the whole system when it is connected with the solar collector. In building the model, the following assumptions were made:

- the thermo-physical properties of brackish water are identical to those of pure water;
- the effect of non-condensable gases released from water when it is heated or expanded can be neglected;
- the system is adiabatic so heat losses are negligible;
- the system processes work under steady-state conditions for each time step;
- the system is working under atmospheric pressure;
- there is no phase change inside the humidifier; and
- the system has a controlled volume, thus the air mass flow rate is constant.

The model was used to simulate and predict the water production of the desalination system over a 24 h period, on the basis of the heat supply during daylight hours with variable solar isolations (W/m^2).

The energy-conservation equations are expressed as given in the following sections.

5.1 Input energy

The consumed energy in the system includes the energy required by the solar collector and the electric heater in addition to the auxiliary components, such as circulation pumps and fans, and it can be expressed as:

$$\dot{Q}_{\text{input}} = \dot{Q}_{\text{hum}} + \dot{Q}_{\text{aux}} \tag{1}$$

where $\dot{Q}_{\text{hum}}$ is the supplied energy at the humidifier chamber and $\dot{Q}_{\text{aux}}$ is the auxiliary energy required by the circulation pumps and the fans in the system.

- The energy supplied to the humidifier

$$\dot{Q}_{\text{hum}} = \dot{m}_{\text{w,h}} C_{\text{p}} (T_{\text{h,i}} - T_{\text{h,o}}) \tag{2}$$

$$\dot{Q}_{\text{hum}} = \dot{Q}_{\text{col}} + \dot{Q}_{\text{heater}} - \Delta \dot{Q}_{\text{losses}} \tag{3}$$

where $\dot{m}_{\text{w,h}}$ is mass flow rate of hot water sprayed into humidifier, C_{p} is specific heat of water and $T_{\text{h,i}}$ and $T_{\text{h,o}}$ are the temperatures of water at inlet and outlet of humidifier, respectively.

5.2 The output energy

The output energy can be expressed in terms of the condensation energy, which equals the latent heat of condensation shown in the following equation:

$$\dot{Q}_{out} = h_{fg} * W_p \tag{4}$$

where h_{fg} is the latent heat of condensation and W_p is the rate of produced potable water. It can be expressed as in the following equation:

$$W_p = \dot{m}_a(\omega_3 - \omega_4) \tag{5}$$

where $\dot{m}_a$ is the mass flow rate of air and ω_3 and ω_4 are the specific humidities of the water at the inlet and the outlet of the dehumidification chamber, respectively.

In this stage, it was assumed that the heat losses in the desalination unit are negligible (the diabetic wall condition).

The dependence of the latent heat of water condensation on the temperatures was given as proposed by Cooper [18]:

$$h_{fg}(T) = 1000 \times [3161.5 - 2.40741(T_{h,i} + 273)]. \tag{6}$$

The specific heat of water is defined as a function of its temperature as suggested by Eames *et al.* [9].

$$C_p = 1000 \times [4.2101 - 0.0022T + 5 \times 10^{-5}T^2 - 3 \times 10^{-7}T^3] \tag{7}$$

In these equations, h_{fg} is in J/kg, T in °C and C_p in J/kg °C.

Initially, to carry out the modeling, it was assumed that the temperature difference between the inlet and the outlet of the humidifier for hot water was ~5°C; later it was experimentally proved that the difference in temperature mainly depended on the hot water temperature. Hence, a representative formula was derived from several experimental results and used to refine and validate the model and it was found that it correlated closely with the experimental values with ~95%.

5.3 Humidifier effectiveness

The effectiveness of adiabatic humidification chamber can be calculated according to the following equation:

$$\varepsilon_{hum} = \frac{T_{ai} - T_{ao}}{T_{ai} - T_{ws}} \tag{8}$$

where T_{ai}, T_{ao} and T_{ws} are the dry bulb temperature of the inlet air, dry bulb temperature of the outlet air and the temperature of the wet surface, respectively.

The heat balance equation inside the humidifier is given as:

$$\dot{m}_a(h_{ai} - h_{ao}) = C_{pw}\dot{m}_{wi}T_{wi} - C_{pw}\dot{m}_{wo}T_{wo} \tag{9}$$

where $\dot{m}_a$, $\dot{m}_{wi}$ and $\dot{m}_{wo}$ are the moist air and salt water mass flow rates (kg/h) at the inlet and the outlet of the humidifier, respectively, T_{wi} and T_{wo} are the water temperatures for the inlet and the outlet of the humidifier, respectively, in °C, C_{pw} is the specific heat (kJ/kg °C) of water and h_a, enthalpy of moist air in kJ/kg.

The effects of different ratios of water to air mass flow rates were investigated to measure the efficiency of the humidification process in addition to the dependency of the efficiency on the air velocity in the humidification chamber. It was found that the effectiveness of the tested humidifier could reach ~99%, and therefore it was assumed that the air at point 3 is fully saturated.

5.4 Dehumidifier

The efficiency of the condenser heat exchanger can be defined as the latent heat of condensation given to the circulated cooling water through the condenser (dehumidifier) to the input heat energy, as shown in the following formulas:

- The heat input into the condenser through the vapor air is

$$Q_{Input} = \dot{m}_a(h_{a3} - h_{a4}) \tag{10}$$

  where h_{a3}, h_{a4} and $\dot{m}_a$ are the water vapor enthalpies at the inlet and the outlet of the condenser and the air mass flow rate, respectively.
- Heat energy balance across the dehumidifier is

$$\dot{m}_a(h_{a3} - h_{a4}) = \dot{m}_{cw}C_p(T_{w2} - T_{w1}) + W_pC_pT_{distillate} \tag{11}$$

  where T_{w2}, T_{w1} and $\dot{m}_{cw}$ are the water temperatures of the cooling water at the outlet and the inlet of the condenser pipe and the cooling water mass flow rate, respectively and W_p and $T_{distillate}$ are the rate and the temperature of the fresh water distillate.

5.5 Solar collector efficiency

The solar collector efficiency can be defined in terms of the inlet and the outlet fluid temperatures of the collector manifold, the area of the collector and the mass flow rate as suggested by Yuan and Zhang [7].

$$\eta_i = \frac{\dot{m}_c C_p(T_{SCi} - T_{SCo})}{\bar{G}A_{col}} \tag{12}$$

The efficiency of the evacuated solar collector used can be also represented as in [19].

$$\eta_i = 0.84 - 2.02\frac{T_m - T_a}{\bar{G}} - 0.0046\bar{G}\left[\frac{T_m - T_a}{\bar{G}}\right]^2 \tag{13}$$

where T_m is the mean collector temperature, $T_m = ((T_{SCi} + T_{SCo})/2)$ (in °C). T_a is the ambient air temperature (°C) and $\bar{G}$ is the solar irradiance (W/m^2)

5.6 Storage tank

In this model, a water storage tank was incorporated into the system to allow the system to run for 24 h. A completely mixed storage tank is assumed.

The energy balance equation for the storage tank with a solar collector heat exchanger is [4].

$$M_s C_{ps} \frac{dT_s}{dt} = \dot{Q}_{col} - \dot{Q}_{losses} - \dot{Q}_{hum} \quad (14)$$

$$M_s C_{ps} \frac{dT_s}{dt} = \dot{m}_{w,h} C_p (T_{h,o} - T_s) + \dot{m}_c C_p (T_{SCi} - T_{SCo} \quad (15)$$

where $\dot{m}_{w,h}$ and $\dot{m}_c$ are the mass flow rate of hot water sprayed in the humidifier and through the solar collector, respectively and C_p is the specific heat of water. $T_s = T_{h,i}$ and $T_{h,o}$, where $T_{h,i}$ and $T_{h,o}$ are the temperatures of the water at the inlet and the outlet of the humidifier.

5.7 Psychometric definitions and formulas

The psychometric parameters were calculated for the analysis of the desalination system of humidification and dehumidification on the basis of the formulas obtained from ASHRAE 1997 Hand book Fundamentals and Hyland and Wexler's [20] formulas:

- Specific humidity

$$\omega = 0.62198 \left(\frac{P_s}{P_i - P_s} \right) \quad (16)$$

$$p_s = e^{(25.5771 - [4042.9/(T_s - 37.58)])} \quad (17)$$

In these equations the temperature is in °C and pressure is in Pa.

- Relative Humidity (RH)

$$RH = \frac{P_w}{P_{ws}} \quad (18)$$

- Enthalpy of moist air (h)

$$h = C_{pa} T_i + \omega (2501 + 1.805T)_i \quad (19)$$

6. RESULTS AND ANALYSIS

6.1 Modeling and simulation

The experimental investigation and theoretical work were conducted to assess the performance when solar energy is used for sea water desalination. The effect of the different working parameters on the production of fresh water was also investigated.

The developed mathematical model describing the water desalination processes was programmed initially using the Engineering Equation Solver software (EES, 2012) and due to the limitation of EES in a continuous transient simulation. A computer Matlab simulink simulation program was developed for simulation and optimization of system performance. In this program, energy and mass balance equations and boundary conditions are solved simultaneously using the analytical methods as described above. The mathematical model has been validated using the experimental results and for this purpose a comparison between the experimental and the theoretical results has been conducted. The experimental and theoretical values for the temperatures and total daily distillate output were found to be closely correlated, as shown in Figure 6. The accuracy between the measured and simulated temperatures inside the storage tank ranged from 93.9 to 99%. The validated model was then used to investigate the effects on the productivity of potable water of different design parameters such as temperatures, mass flow rates and solar insolation under different climatic conditions in the Middle East for summer, spring, autumn and winter. Figure 7 shows that the average daily water production of the system in summer,

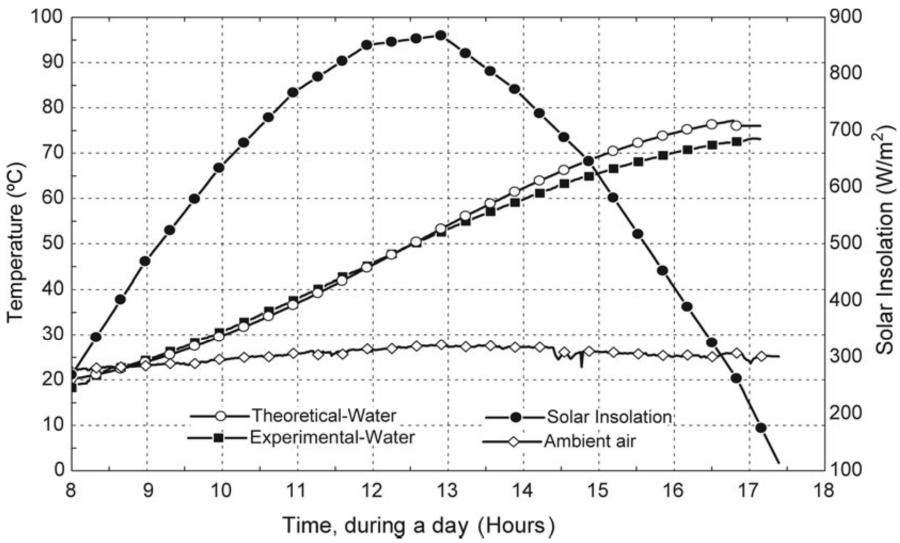

Figure 6. *Water temperature inside the storage tank under simulated solar radiation for a spring day in the Middle East.*

spring, autumn and winter is 32, 25.5, 23.7 and 15.8 kg per day, respectively, with an average annual daily production of 24 kg/day. This amount of fresh water could be sufficient for a family of five persons for drinking and cooking purposes.

Figures 8 and 9 show the variations of simulated water production and temperature inside the water desalination system for the spring season with different sizes of solar collector. It can be seen that the solar energy was stored during the day in a storage tank and, after sunset, the desalination unit was switched on to produce fresh water. The desalination system was simulated for two operational schemes. In the first scheme, the solar energy delivered by the solar collector is stored in the saline water in the storage tank during the daylight period from 7:00 am until 5:00 pm without water circulation into the desalination system and then the desalination system is started and it operates during the night. In the second system, the saline water in the storage tank is heated by solar energy from 7:00 am until 1:00 pm and then the desalination system is started to produce fresh water. The first scheme is preferred because it allows the saline water to reach a temperature of >65°C, which eliminates the need for any further biological treatment of the distillate.

It can be seen from Figure 9 that during spring time, the highest temperature obtained in the water tank connected with a 2.5 m^2 solar collector is 92°C in the first operational scheme. However, the simulation of solar insolations in summer showed that the temperature of saline water reached 100°C. Therefore, during summer time, it is recommended that the second operational scheme be adopted in order to avoid excessive temperatures and reduce the heat losses during the energy-storage period. Operating the desalination system with saline water temperatures between 60 and 80°C would also eliminate salt scaling.

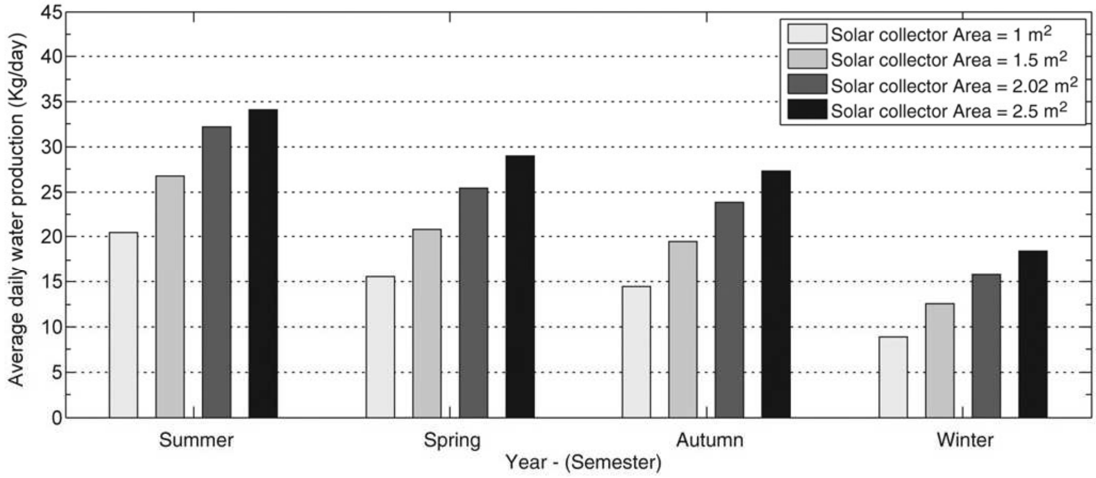

Figure 7. *Simulated desalinated water production for annual solar insolation variations in the Middle East.*

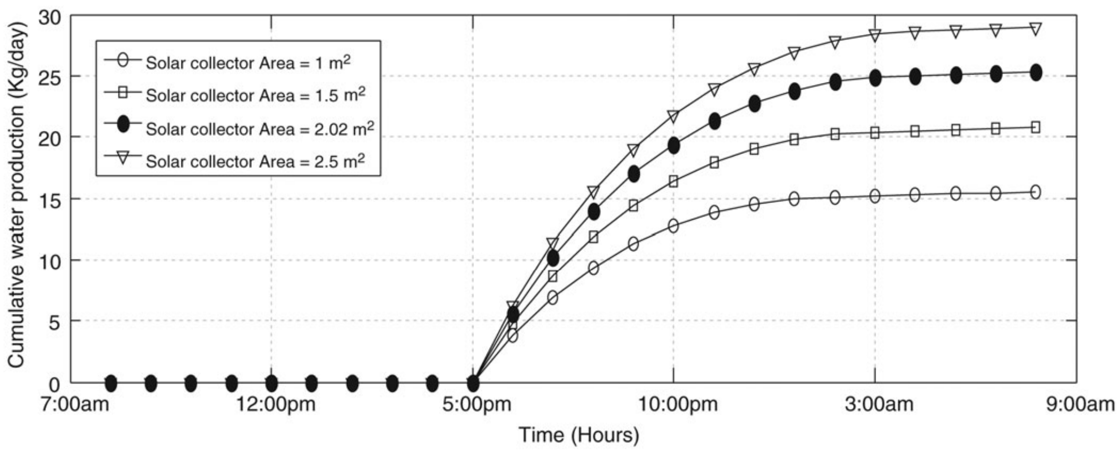

Figure 8. *Fresh water production as a function of solar collector size for a spring day in the Middle East.*

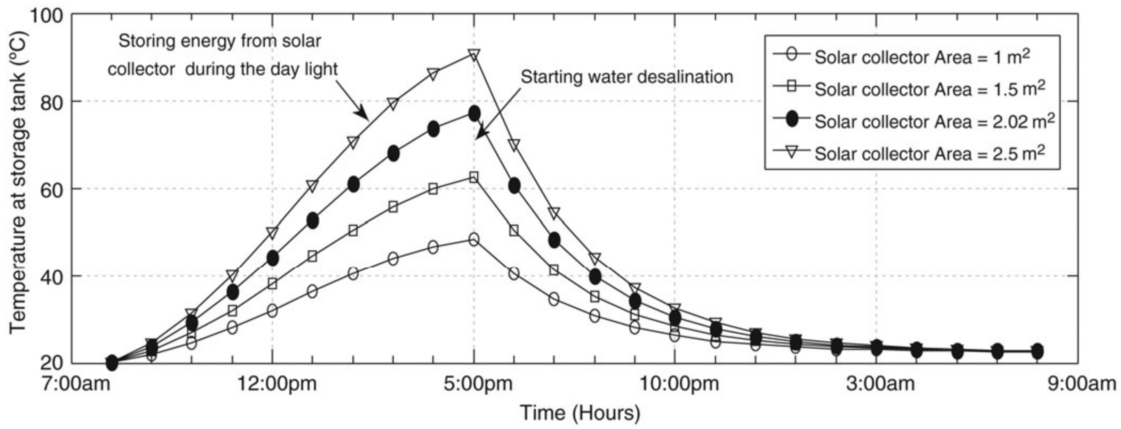

Figure 9. *Temperature variations for the solar energy storing and water desalination process inside the desalination system with different solar collector areas.*

Hence, the desalination system should be operated according to the first scheme during spring, autumn and winter, but the second operational scheme is more suitable for the summer.

The simulation results of the desalination unit for two operational schemes under the Middle East climatic conditions show that a solar collector with an area of 2.02 m^2 is the most appropriate size for the desalination unit. This system configuration was tested under the second scheme during summer time and it was found that the saline water reached a maximum temperature of 65°C, which is suitable for the water desalination process, and water production was higher—~32 kg/day compared with 26 kg/day in the first operational scheme—because the solar energy is utilized instantaneously and there is less heat loss during the storage time.

6.2 Experimental results

6.1.1 *Temperature and relative humidity*

Figure 10 presents the temperature variations inside the desalination system at different locations. It can be seen that the maximum temperature difference between the inlet and the outlet of the humidifier during the hot water circulation process was ~6–11°C. It can be seen also that the desalination system reached the steady state 45–60 min after hot water circulation.

Then the air at the top of the humidifier became fully saturated and the humidity sensors got wet and faulty. To overcome this problem, dry and wet bulb temperature sensors were then used to calculate the relative humidity and ensure that the air at point 3 had become completely saturated.

Figures 11 presents the variations of measured relative humidity in the system. The relative humidity achieved at point 3 was 90% at the beginning of operation and it increased gradually until it reached the saturation point within 60 min when the supplied hot water temperature was >55°C. Meanwhile, the relative humidity of the exhaust air at point 4 varied between 90 and 100%. It can be seen that the relative humidity of the ambient air varied, according to the lab conditions, from 50 to 75% with an ambient dry bulb temperature of ~23–25°C, as shown in Figure 10.

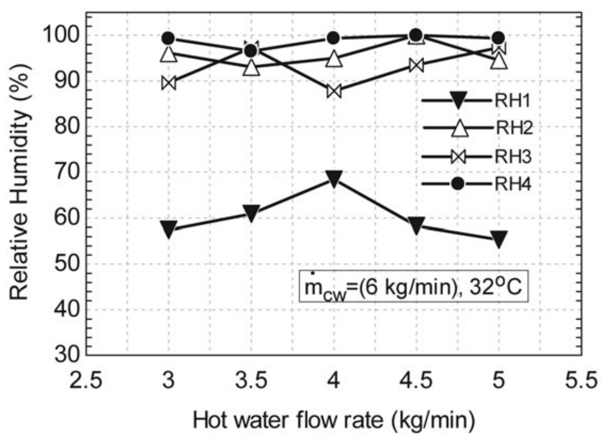

Figure 10. *Variation of relative humidity at different locations in the desalination system.*

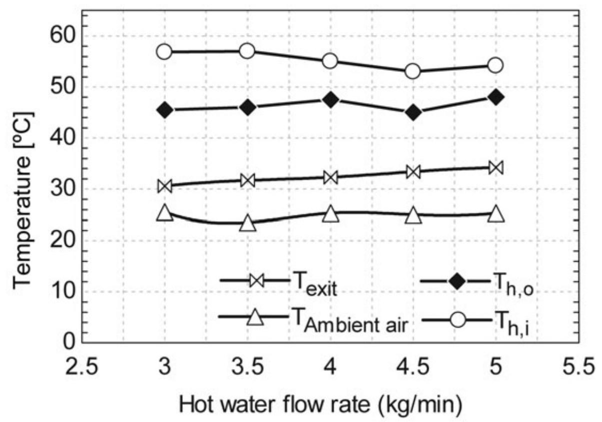

Figure 11. *Temperature variations in the desalination unit.*

6.1.2 *Air mass flow rate*

A constant mass flow rate of air is supplied from the fan. As the air temperature increases, the air becomes less dense at constant volume; hence, more mass is supplied as the temperature increases. The measured values showed a relatively constant air flow rate of 2.5–3.1 kg/min, as shown in Figure 12.

Subsequently, the desalination system was investigated with different air mass flow rates using a high-speed fan with a variable mass flow regulator. It was found that water productivity increased significantly as the air mass flow rate increased until it became constant at a certain point.

6.1.3 *Water production*

Figure 13 shows the water productivity as a function of hot water mass flow rate. It was found that the higher the mass flow rate, the greater the water productivity at a certain optimum cooling water mass flow rate. In order to fulfill this condition, the system was tested under different mass flow rates and a minimum ratio of hot water to cooling water was optimized. The experimental results showed that the minimum ratio should not be <0.7 while the optimal ratio was 1.1, the latter producing a larger coefficient of performance (COP) of ∼1.425 and a water production of 4.68 kg/h, as illustrated in Figure 14.

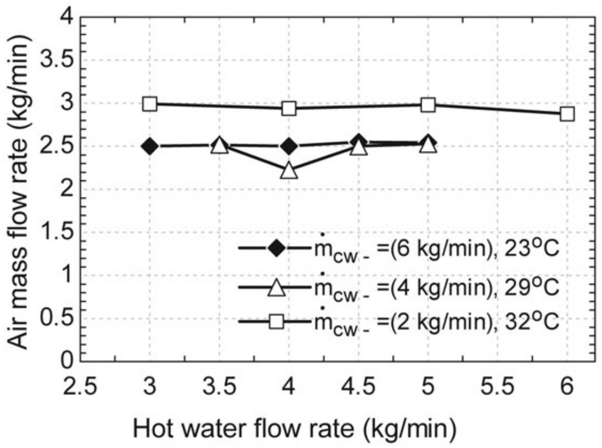

Figure 12. *Variations of measured air mass flow rates.*

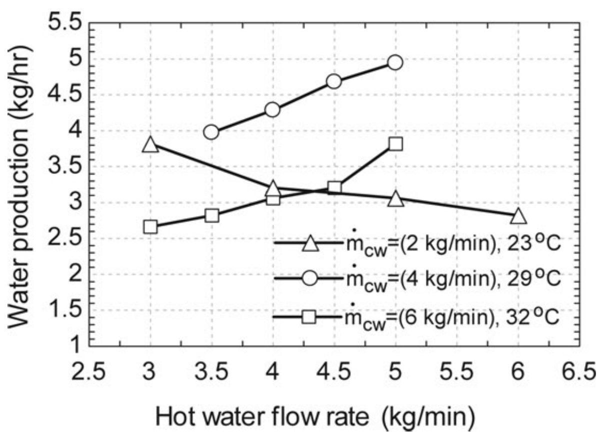

Figure 13. *Water production as a function of hot water mass flow rates.*

Figure 14 shows the COP variation with the change of hot water mass flow rate from 3 to 6 kg/min at constant circulation mass flow rate of salty cooling water into the dehumidifier of values equal to 2, 4 and 6 kg/min. It can be also seen in Figure 15 that the COP obtained ranged from 0.82 to 1.41 at optimal mass flow rate ratio of hot to cooling water of 1.1. This ratio has a significant effect on the COP values and water productivity.

6.1.4 *Humidifier efficiency*

The efficiency of the humidifier is significantly affected by the inlet hot water temperature and the relative humidity and for this reason several tests were carried out and the humidifier effectiveness was calculated as described in Figure 16. The results indicated that the humidifier efficiency is linearly proportional to the magnitude of relative humidity at the humidifier, as shown in Figure 17. It can be noted that the efficiency of the humidifier can reach 99% when the relative humidity is 98–100% and this can be achieved 60 min after operation when the system reaches the steady-state condition.

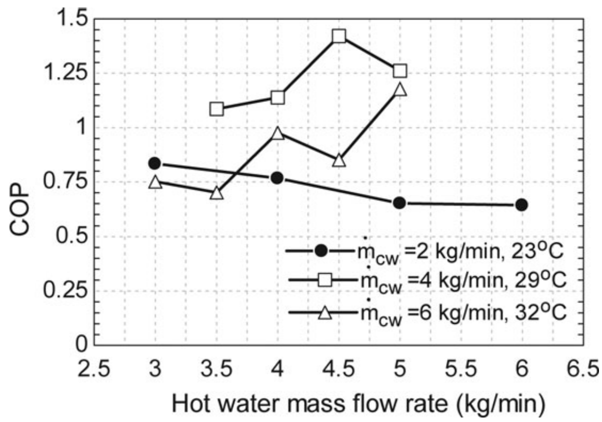

Figure 14. *The relationship between the COP and hot water mass flow rate.*

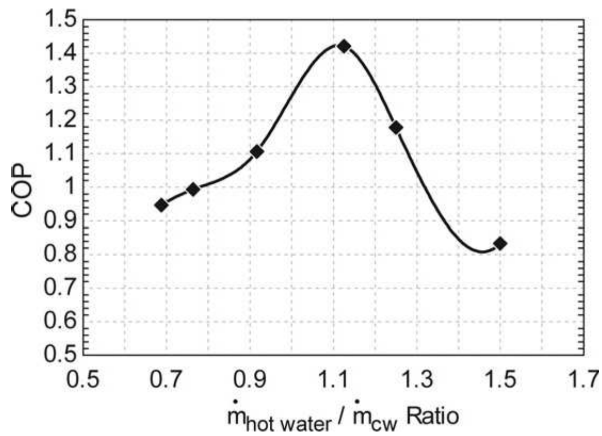

Figure 15. *The relationship between COP and hot water and cooling water mass flow rate ratio.*

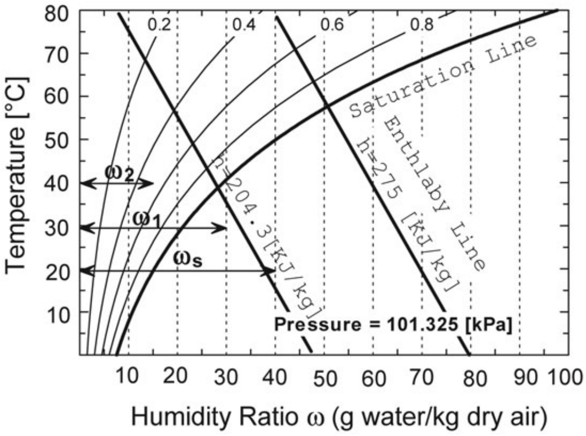

Figure 16. *Humidification efficiency definition.*

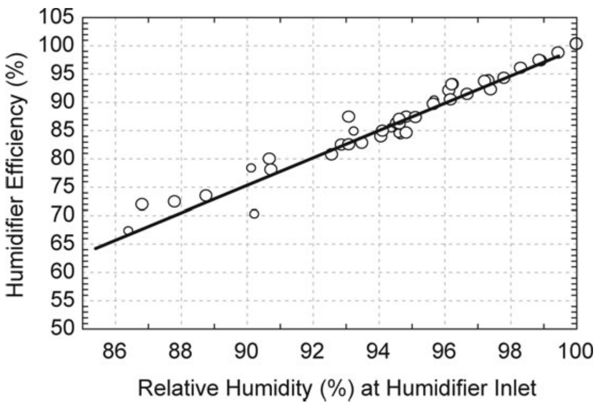

Figure 17. *The experimental results of the effect of relative humidity on humidification chamber efficiency.*

7. CONCLUSIONS

An innovative and efficient solar water desalination system based on the humidification and dehumidification concept was investigated. A natural-circulation electric water heater was used as a heat source and an evacuated solar collector panel was incorporated into the system for experimental and theoretical work. The experimental results showed that the productivity of the system was significantly affected by the temperature of the saline water to be desalinated and the air mass flow rate. The system produced 7 kg/h of fresh water when the input saline water was 55–60°C. The highest COP obtained was ~1.42 with a continuous heater with a capacity of 2.5 kWh. This value of the COP is higher than in similar previous work conducted with the same concept and in conventional solar distillation systems such as solar stills coupled with a solar collector. Running the system coupled with an evacuated solar collector in summer can produce up to 16 kg/m^2/day, which is significantly higher than fresh water produced by an evacuated tube solar collector four-stage still system and found to be ~5 kg/m^2/day [21]. The experimental tests and theoretical simulation proved that when the system is operated at a higher temperature (60–70°C), the fresh water produced is of a high quality and well within the World Health Organization guidelines for satisfactory drinking water so there is no need for post treatment to prevent biological contamination. The evacuated solar collector provided 69% efficiency for heating the input water. It was noted that the cost of running this solar-powered system is more economically viable than those operated by electricity from the grid. Further tests will be conducted to investigate the system under real outdoor conditions in the Middle East. The system could make a significant contribution to reducing potable water shortages, especially in Africa, the Middle East and China, when coupled with solar collectors or a heat pump operated by photovoltaic cells.

Acknowledgments

The authors gratefully acknowledge that this research was partially supported by the Institute of Sustainable Energy Technology, University of Nottingham and the Islamic Development Bank—PhD scholarship.

References

[1] United Nations Environment Programme. http://www.unep.org/themes/freshwater.html (10 April 2008, date last accessed).

[2] Al-Kharabsheh S. *Theoretical and Experimental Analysis of Water Desalination System Using Low Grade Solar Heat.*, USA: PhD dissertation—University of FloridaUSA 2003.

[3] Buros OK. *The ABCs of Desalting*. Massachusetts: USA International Desalination AssociationMassachusetts 1999.

[4] Buzás J, Farkas I, Biró A, *et al.* Modelling and simulation aspects of a solar hot water system *Math Comput Simulation* 1998;**48**:33–46.

[5] Abkr A, Ismail A. Theoretical and experimental investigation of a novel multistage evacuated solar still. *J Sol Energy Eng* 2005;**127**:381–385.

[6] Solar Distillation. Practical Action Technology Challenging Poverty, from http://www.practicalaction.org/practicalanswers/product_info.php?products_id=165 (26 October 2007, date last accessed).

[7] Yuan G, Zhang H. Mathematical modeling of a closed circulation solar desalination unit with humidification-dehumidification. *Desalination* 2007;**205**:156–162.

[8] Mohamed AMI, El-Minshawy NA. Theoretical investigation of solar humidification–dehumidification desalination system using parabolic trough concentrators. *Energy Convers Manag* 2011;**52**:3112–3119.

[9] Eames IW, Maidment GG, Lalzad AK. A theoretical and experimental investigation of a small-scale solar-powered barometric desalination system. *Appl Therm Eng* 2007;**27**:1951–1959.

[10] Mohamed AMI, El-Minshawy NAS. Humidification–dehumidification desalination system driven by geothermal energy. *Desalination* 2009;**249**:602–608.

[11] Gude VG, Nirmalakhandan N, Deng S, *et al.* Low temperature desalination using solar collectors augmented by thermal energy storage. *Appl Energy* 2012;**91**:466–474.

[12] Hou S, Zhang H. A hybrid desalination process of a multi effect humidification dehumidification and basin type unit. *Desalination* 2008;**220**:552–557.

[13] Garg HP, Adhikari RS, Kumar R. Experimental design and computer simulation of multi-effect humidification (MEH)-dehumidification solar distillation. *Desalination* 2003;**153**:81–86.

[14] Müller-Holst H, Engelhardt M, Schölkopf W. Small-scale thermal seawater desalination simulation and optimization of system design. *Desalination* 1999;**122**:255–262.

[15] Soufari M, Zamen M, Amidpour M. Performance optimization of the humidification–dehumidification desalination process using mathematical programming. *Desalination* 2009;**237**:305–317.

[16] Farid M, Nawayseh N, Al-Hallaj S, *et al*. 'Solar desalination with humidification/dehumidification process: Studies of heat and mass transfer'. *Proceedings Conference: SOLAR 95*, Hobart, Tasmania, 1995, pp. 293–306.

[17] Al-Hallaj S, Farid MM, Rahman T. Solar desalination with a humidification-dehumidification cycle: performance of the unit. *Desalination* 1998;**120**:273–280.

[18] Cooper PI. The absorption of radiation in solar stills. *Sol Energy* 1969;**12**:333–346.

[19] MAZDON® HP200. Evacuated Tube Solar Energy Collector. Technical Reference & Installation Manual Domestic Hot Water. http://www.solarthermal.com (31 December 2011, date last accessed).

[20] Wessel DJ. ASHRAE Fundamentals Handbook 2001 (SI Edition). *American Society of Heating, Refrigerating, and Air-conditioning Engineers* 2001.

[21] Shatat MIM, Mahkamov K. Determination of rational design parameters of a multi-stage solar water desalination still using transient mathematical modelling. *Renew Energy* 2010;**35**:52–61.